

Dark-gap solitons with mixed nonlinear and linear lattices

Xue-Fei Zhang(张雪菲), Xiao-Yang Wang(王笑阳), Hui-Lian Wei(魏慧莲), and Tian-Fu Xu(徐天赋)
Citation: Chin. Phys. B, 2025, 34 (**8**): 080303. DOI: 10.1088/1674-1056/add4dd
http://cpb.iphy.ac.cn; http://iopscience.iop.org/cpb

What follows is a list of articles you may be interested in

Surface solitons in Kerr-type nonlinear media with chirped lattices

Xiaoyang Wang(王笑阳), Huilian Wei(魏慧莲), Xuefei Zhang(张雪菲), and Tianfu Xu(徐天赋)
Chin. Phys. B, 2025, 34 (**6**): 060302. DOI: 10.1088/1674-1056/adc083

Periodic modulation of adiabatic dynamics in non-reciprocal Landau-Zener systems

Rong Chang(常蓉) and Sheng-Chang Li(栗生长)
Chin. Phys. B, 2025, 34 (**3**): 030305. DOI: 10.1088/1674-1056/adab64

Coulomb-assisted nonlocal electron transport between two pairs of Majorana bound states in a superconducting island

Hao-Di Wang(王浩迪), Jun-Tong Ren(任俊潼), Hai-Feng Lü(吕海峰), and Sha-Sha Ke(柯莎莎)
Chin. Phys. B, 2024, 33 (**5**): 050310. DOI: 10.1088/1674-1056/ad2a68

Coherence of nonlinear Bloch dynamics of Bose—Einstein condensates in deep optical lattices

Ai-Xia Zhang(张爱霞), Wei Zhang(张薇), Jie Wang(王杰), Xiao-Wen Hu(胡潇文), Lai-Lai Mi(米来来), and Ju-Kui Xue(薛具奎)
Chin. Phys. B, 2024, 33 (**4**): 040305. DOI: 10.1088/1674-1056/ad1b46

Dynamical nonlinear excitations induced by interaction quench in a two-dimensional box-trapped Bose-Einstein condensate

Zhen-Xia Niu(牛真霞) and Chao Gao(高超)
Chin. Phys. B, 2024, 33 (**2**): 020314. DOI: 10.1088/1674-1056/ad1179

Dark-gap solitons with mixed nonlinear and linear lattices

Xue-Fei Zhang(张雪菲), Xiao-Yang Wang(王笑阳), Hui-Lian Wei(魏慧莲), and Tian-Fu Xu(徐天赋)†

Hebei Key Laboratory of Microstructural Material Physics, School of Science, Yanshan University, Qinhuangdao 066004, *China*

(Received 21 February 2025; revised manuscript received 11 April 2025; accepted manuscript online 7 May 2025)

We study the existence and stability of dark-gap solitons in linear lattice and nonlinear lattices. The results indicate that the combination of linear and nonlinear lattices gives dark-gap solitons unique properties. The linear lattice can stabilize dark-gap solitons, while the nonlinear lattice reduces the stability of dark-gap solitons. On the basis of numerical analysis, we investigate the effects of lattice depth, chemical potential, nonlinear lattice amplitude, and nonlinear lattice period on the soliton in mixed lattices with the same and different periods. The stability of dark-gap soliton is studied carefully by means of real-time evolution and linear stability analysis. Dark-gap solitons can exist stably in the band gap, but the solitons formed by the mixed lattices are slightly different when the period is the same or different.

Keywords: dark-gap solitons, nonlinear and linear lattices, linear stability analysis

PACS: 03.75.Lm, 42.50.Md, 43.25.Rq

DOI: 10.1088/1674-1056/add4dd **CSTR:** 32038.14.CPB.add4dd

1. Introduction

Solitons, as a special wave phenomenon,[1] have attracted much attention because of their unique self-localization and stability in the field of nonlinear optics[2] and Bose–Einstein condensates (BECs).[3,4] Solitons originate from various nonlinear effects, maintaining their shape and preventing energy dispersion during propagation.[5–7] In recent years, with the rapid development of periodic modulation structural materials such as photonic crystals[8,9] and gratings,[10,11] a new type of solitons, known as the gap solitons, has gradually become a research hotspot. When light pulses or matter waves propagate through media with periodically modulated structures, their frequencies lie within the forbidden bands or gaps formed by the periodic structure.[12,13] At this point, the light pulses or matter waves undergo strong Bragg reflection, interacting with the nonlinear effects of the medium to form gap solitons.[14,15] As an important type of gap solitons, dark-gap solitons have unique energy distribution and formation mechanism.[16–18] Unlike the energy bulge of bright-gap solitons at zero background intensity,[19] dark-gap solitons appear as energy depression at intensity background.[20–23] This kind of energy sag is an inherent feature of strong light transmission in normal dispersive single-mode fiber and is also affected by periodic modulation structure.[24–26] The formation of dark-gap solitons usually has no threshold requirement, and any initial strength depression may gradually evolve into one or more dark-gap solitons. The patterns of bright and dark-gap solitons are well implemented in BECs.[27–32] By contrast, the theoretical study of dark-gap solitons under various models is relatively lacking.

The outer periodic potential[33,34] and the periodic potential nonlinearity[35] give rise to various types of solitons, and their mixed potentials have been extensively studied. Zhang *et al*. investigated the instability of BECs in a mixture of nonlinear and linear lattices.[36] He *et al*. revealed that the combination of $\mathcal{PT}$-symmetric linear and nonlinear lattices has the capacity to stabilize lattice solitons.[37,38] The studies of mixed potential can be realized by means of optical lattice. One of the reasons for the creation of Bloch bands is the optical lattice,[34,39] in which the interatomic interactions are generated by condensed atomic BECs and optical lattices that provide linear periodic potential. The nonlinear lattice[38,40,41] represents a spatially periodic modulation of the interatomic interactions, and it can be experimentally achieved by controlled optical Feschbach resonance. Wang *et al*. proved that dark solitons exist stably in a purely quintic nonlinear lattices.[42] In addition, literatures[43,44] add a constant interaction to the nonlinear term to stabilize the solitons. The effective interaction of atomic repulsion in a nonlinear lattice with constant repulsion provides a possible means for the stability of solitons. As far as we know, dark-gap solitons in the mixed nonlinearity of the periodic potential and the outer periodic potential have not been studied.

In this paper, we introduce the existence and dynamic properties of dark-gap solitons in one-dimensional (1D) linear and nonlinear lattices. Dark-gap solitons with different lattice depths and chemical potentials are studied. Our findings reveal that the lattice depth has a great influence on solitons, and the combination of linear and nonlinear lattices serves to stabilize the dark-gap solitons. The stability of these solitons

†Corresponding author. E-mail: tfxu@ysu.edu.cn

© 2025 Chinese Physical Society and IOP Publishing Ltd. All rights, including for text and data mining, AI training, and similar technologies, are reserved.

is validated through both linear stability analysis method and real-time evolution method.

The structure of this paper is as follows: In Section 2, we present a model of dark-gap solitons in BECs, find solitons by specific methods, and evaluate the stability of these solitons by two different methods. In Section 3, we use numerical methods to analyze the existence and stability of solitons at different lattice depths and chemical potentials. Finally, in Section 4, we give a brief summary of our findings.

2. Model and methods

In the framework of the mean-field approximation, the dynamical behavior of the BECs can be described by the following nonlinear Gross–Pitaevskii equation (GPE):[36,44,45]

$$\mathrm{i}\hbar\frac{\partial\Psi}{\partial t}=\left[-\frac{\hbar^2}{2m}\nabla^2+V(r)+W_{\mathrm{non}}|\Psi|^2\right]\Psi, \tag{1}$$

where ∇^2, $\hbar$, t, and m denote the Laplace operator, Planck's constant, evolution time, and the mass of atom, respectively. $\Psi(r,t)$ denotes the macroscopic wave function of the condensate, $V(r)$ is the experimentally generated optical lattice potential field, $r=(x,y,z)$ is a Cartesian coordinate vector, and the nonlinear coefficient is $W_{\mathrm{non}}=g_1+W$. $g_1=4\pi\hbar^2a_{\mathrm{s}}/m$ is the two-body interaction strength, here a_{s} denotes the s-wave scattering length ($a_{\mathrm{s}}>0$ corresponds to repulsive interactions, and $a_{\mathrm{s}}<0$ corresponds to attractive interactions). W denotes the nonlinear interaction strength modulated with spatial periodicity.

In experimental studies,[46,47] the BECs are usually imprisoned in a harmonic oscillator potential well described by $V(r)=(m/2)(\omega_x{}^2x^2+\omega_y{}^2y^2+\omega_z{}^2z^2)$, where ω_x, ω_y, and ω_z correspond to the binding frequencies in the three spatial dimensions of x, y, and z, respectively. When $\omega_y=\omega_z$ and $\omega_z\gg\omega_x$, the BEC is strongly constrained in the y- and z-directions, forming a cigar-shaped distribution along the x-direction, and the three-dimensional (3D) GPE can be simplified to 1D GPE ($\omega_x=2\pi\times10$ Hz, $\omega_y=\omega_z=2\pi\times200$ Hz in Ref. [48]). This paper specialises in the 1D GPE. The length, time, wave function and intensity of the interaction of two bodies are dimensionless by introducing dimensionless parameters: $\tilde{t}=\omega_x t$, $\tilde{x}=x/a_{\mathrm{ho}}$, $\tilde{\Psi}=\sqrt{a_{\mathrm{ho}}{}^3/n_0}\Psi$, $\tilde{g_1}=2a_sn_0\sqrt{\omega_z\omega_y}/a_{\mathrm{ho}}\omega_x$, where $a_{\mathrm{ho}}=\sqrt{\hbar/m\omega_x}$ is the harmonic oscillator characteristic length. $n_0=N$ is the given particle number density.

The dimensionless GPE is used to describe BECs system with 1D linear lattice and nonlinear lattice:

$$\mathrm{i}\frac{\partial\Psi}{\partial t}=-\frac{1}{2}\frac{\partial^2\Psi}{\partial x^2}+V\Psi+g_1|\Psi|^2\Psi+W|\Psi|^2\Psi. \tag{2}$$

The linear lattice is $V=v_0\sin^2(x)$, v_0 is the linear lattice depth. $W=w_0\cos(x)$ is the nonlinear lattice, and w_0 is the nonlinear lattice amplitude. In this paper, $g_1=1.0$ is taken to produce a repulsive interaction.

The stable solution of Eq. (2) can be defined as $\Psi(x,t)=\psi(x)\exp(-\mathrm{i}\mu t)$, which $\psi(x)$ is a complex-valued function, and μ is a chemical potentical. By substituting $\Psi(x,t)$ into Eq. (2), we obtain the stationary Schrödinger equation as follows:

$$-\mu\psi-\frac{1}{2}\frac{\partial^2\psi}{\partial x^2}+V\psi+|\psi|^2\psi+W|\psi|^2\psi=0. \tag{3}$$

The solution of the stationary equation can be obtained by Newton's iteration.[49] The dark-gap soliton is in the linear band gap, so the linear part of Eq. (3) as follows:

$$-\mu\psi-\frac{1}{2}\frac{\partial^2\psi}{\partial x^2}+V\psi=0. \tag{4}$$

Due to the periodicity of the linear lattice, we can define $\psi(x)=\phi_k(x)\exp(-\mathrm{i}kx)$ by Bloch's theorem, where k is the Bloch wave number, and $\phi_k(x)$ is a periodic function with $\phi_k(x)=\phi_k(x+\pi)$. In addition, we replace the periodic linear lattice with plane wave expansion to obtain the Bloch band structure of the linear lattice V. Because of the defect in the number of particles caused by the repulsive nonlinearity, we define the number of defective atoms $N=\int_{-\infty}^{+\infty}(|\psi_{\mathrm{back}}|^2-|\psi|^2)\mathrm{d}x$ in BECs, ψ_{back} is the continuous wave background.

There is a question worth studying that dark-gap solitons exist stably in BECs system. We use two different methods to prove the stability of dark-gap solitons. The first method is linear stability analysis,[50] add a perturbation at $\psi(x)$, as follows:

$$\begin{aligned}\Psi(x,t)\ =\ &[\psi(x)+p(x)\exp(\delta t)+q^*(x)\exp(\delta^* t)]\\&\times\exp(-\mathrm{i}\mu t),\end{aligned} \tag{5}$$

where $p(x)$ and $q(x)$ are small perturbations. Substituting Eq. (5) into Eq. (2) to obtain the eigenvalue problem

$$\mathrm{i}\delta\begin{pmatrix}p\\q\end{pmatrix}=\begin{pmatrix}L&(1+W)\psi^2\\-(1+W)\psi^{*2}&-L\end{pmatrix}\begin{pmatrix}p\\q\end{pmatrix}, \tag{6}$$

where

$$L=-\mu-\frac{1}{2}\frac{\partial^2\psi}{\partial x^2}+V+2(1+W)|\psi|^2.$$

If the real part of the eigenvalue is zero, the soliton solution is stable. Otherwise, it is unstable. The second method is to add 10% random noise to the solution initial wave function ψ as an initial condition for Eq. (2), and then to numerically monitor its evolution.[51] If its deviation from $\psi(x)$ is constant with the development of the system, the solution $\psi(x)$ is stable; on the contrary, it is unstable.

3. Numerical results and analysis

In this section, we use different periodic spatial distributions for linear and nonlinear regions. First, the nonlinear lattice is $W = w_0\cos(x)$. The linear lattice V has a period of π and the nonlinear lattice W has a period of 2π, so mixed lattices period is 2π. We fix the linear lattice depth $v_0 = 3.0$ to explore the effects of different periodic spatial distributions on dark-gap solitons, and whether they can propagate stably. Substitute the linear lattice V into Eq. (4) to get the Bloch band of the linear lattice, as shown in Fig. 1. The spectral gap located between two adjacent Bloch bands opens and widens as the linear lattice depth v_0 increases in Fig. 1(a). Figure 1(b) shows the corresponding band gap structure for $v_0 = 3.0$. Solitons may exist stably in band gaps, so we are interested in the first band gap and the second band gap. In this paper, dark-gap solitons are studied along the dotted line from bottom to top.

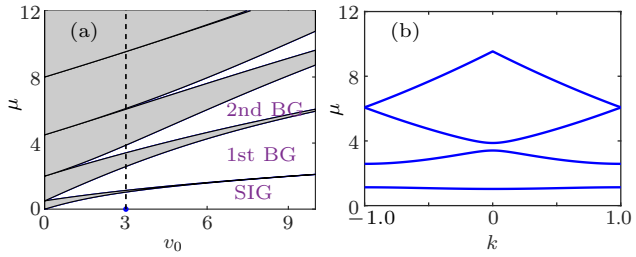


Fig. 1. The Bloch band structure of linear lattice. (a) Linear lattice with lattice depth v_0 as a variable. (b) Band gap structure at $v_0 = 3.0$. The blank spaces represent the band gaps, and shaded areas represent Bloch bands. SIG and 1st (2nd) BG are semi-infinite band gap, first (second) band gap.

Black dotted line in Fig. 2(c) shows a uniformly distributed continuous wave of dark-gap solitons before forming defects. The background wave has a period of 2π. A period has two amplitudes, one large amplitude and one small amplitude. When the linear lattice depth increases, the amplitude of the background decreases. As the chemical potential increases, so does the background amplitude. The excitation of dark-gap solitons not only leads to the trough formed by local density loss, but also accompanies phase jump on both sides of the trough. When the minimum value of density loss is zero, the phase difference caused by phase jump is π. The soliton profile of the fundamental dark-gap solitons are given in Fig. 2(a). Let us use Δ_L to represent the total distance of cup-shaped portion, and Δ_l to denote the separation distance between adjacent dark-gap of the cup-shaped portion. The total separation distance is $\Delta_L = \pi$. The cup-shaped portion of fundamental dark-gap solitons not only decreases with the increase of chemical potential, but also increases with the increase of linear lattice depth.

We continue to study the shape of multipole dark-gap solitons. Multipole dark-gap solitons are formed by the superposition of several fundamental dark-gap soliton modes. Tripole dark-gap soliton is a superposition of three fundamental dark-gap soliton modes in Fig. 2(b). The total distance of its cup-shaped portion is $\Delta_L = 3\pi$, and the separation distance between adjacent dark-gap solitons is $\Delta_l = \pi$. In the same way, the fivepole dark-gap soliton consists of a superposition of five solitons, and the total distance of the cup-shaped portion is $\Delta_L = 5\pi$. Their amplitudes and cup-shaped portions change in the same way that fundamental dark-gap solitons do. The total distance of cup-shaped portion depends on its number of poles.

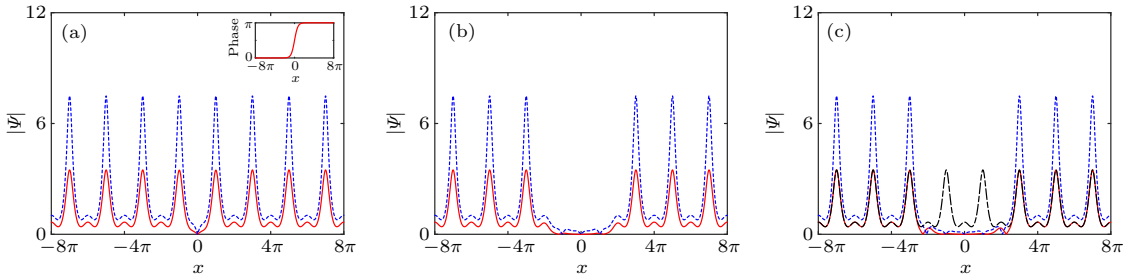


Fig. 2. Dark-gap soliton profile and continuous wave background (dashed black line). Panel (a): fundamental dark-gap solitons, panel (b): tripolar dark gap solitons, panel (c): fivepole dark-gap solitons. The parameters are $v_0 = 3.0$, $w_0 = 1.0$, $\mu = 1.50$ (solid red line), and $\mu = 2.50$ (dotted blue line).

Figure 3(a) shows the relationship between the defective atomic number N of the dark-gap solitons and the chemical potential μ supported by linear lattice. We can clearly see that N and μ show a monotonically increasing in band gaps. The slope of fundamental dark-gap solitons in the first band gap is higher than the slope of the second band gap, but the slope of multipole dark-gap solitons is flatter in the interval. Moreover, the number of defective atoms of multipole dark-gap solitons is dozens of times greater than that of fundamental dark-gap solitons. We also find that dark-gap solitons also conform to the empirical anti-Vakhitov–Kolokolov (anti-VK) stability criterion, which states that $\mathrm{d}N/\mathrm{d}\mu > 0$.

Next, we discuss the stability of these dark-gap solitons. The stability of dark-gap solitons in the first and second band gaps is obtained by linear stability analysis of the eigenequation. Figure 3(b) illustrates in detail the dependence between the eigenvalue $\mathrm{Re}(\delta)$ and the chemical potential μ for the fundamental dark-gap solitons. When the linear lattice depth

$v_0 = 3.0$, the fundamental dark-gap solitons are unstable near the edge of the first band gap, and stable in the region at $\mu \geq 1.92$. In the second band gap, the fundamental dark-gap solitons solitons have very strong stability. The tripole dark-gap solitons in the first band gap are partially stable, μ has an unstable region of 1.34 and 1.54, the other regions can be approximately regarded as stable, and there are no stable solitons in the second band gap. The chemical potential of fivepole dark-gap solitons are completely stable between 1.57 and 1.97, and then have a couple of stable solitons on the edge in the fist band gap. There are all unstable solitons in the second band gap.

When the depth of linear lattice is increased $v_0 = 6.0$ in Fig. 4(a), the stability of the fundamental dark-gap solitons in the band gap is enhanced. The stability of the tripole dark-gap solitons in the band gap is improved, with all solitons being stable in the first band gap except for a few on the edges, which are unstable, and some stable solitons appearing in the second band gap. Similarly, as the depth of the linear lattice increases, so does the number of stable fivepole dark-gap solitons in the band gap, but its stable region is narrower than the fundamental and tripole dark-gap solitons. As shown in Fig. 4(b), increasing the nonlinear lattice amplitude to $w_0 = 2.0$, we find that solitons do not exist in the band gap. Next, the period of the nonlinear lattice is varied, and the stability of the dark-gap solitons is reduced. When the period of the nonlinear lattice is $W = w_0 \cos(2x)$. The fundamental gap solitons are stable except the edge of the band gap. The tripole dark-gap solitons are unstable in the first half of the first band gap and stable in the second half, and there is no stable solitons in the second band gap. Similarly, the stability of fivepole dark-gap solitons is similar to that of tripole dark-gap solitons. Therefore, the more soliton superposition there is, the less stable it is. It is also shown that the stability of dark gap solitons is due to the linear lattice.

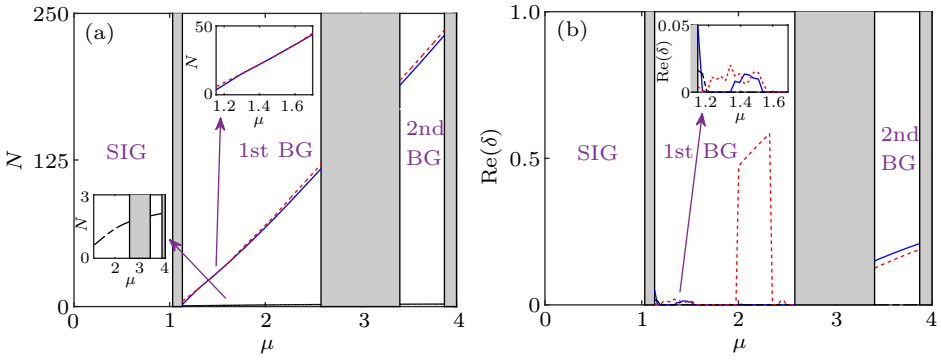


Fig. 3. The defective atomic number N (left) and the real part $\mathrm{Re}(\delta)$ of the eigenvalue (right) *versus* chemical potential μ for dark-gap solitons. The dashed black, solid blue, and dotted red lines represent fundamental dark-gap solitons, tripole dark-gap solitons, and fivepole dark-gap solitons for $v_0 = 3.0$, and $w_0 = 1.0$. The blank area represents the band gap, and the shaded area represents the band. SIG and 1st (2nd) BG are semi-infinite band gap, first (second) band gap.

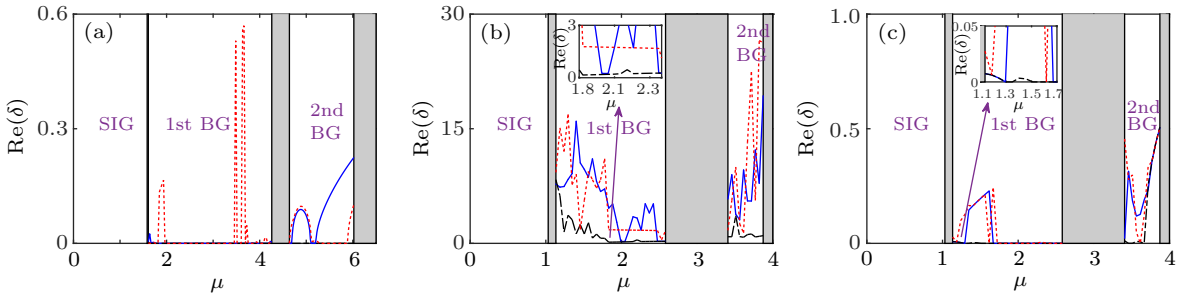


Fig. 4. The relationship between the real part $\mathrm{Re}(\delta)$ of the eigenvalue of dark-gap solitons and the chemical potential μ: (a) $v_0 = 6.0$, $w_0 = 1.0$; (b) $v_0 = 3.0$, $w_0 = 2.0$; (c) $v_0 = 3.0$, $w_0 = 1.0$, $W = w_0 \cos(2x)$.

Now we focus on the dynamic propagation of fundamental dark-gap solitons. Figure 5 shows the propagation of dark-gap solitons in the first band gap and second band gap. We arbitrarily select stable or unstable soliton solutions in Fig. 3(b), showing their solitons profile, linear stability analysis, and real-time evolution graphs. Stable dark-gap solitons maintain their waveforms and amplitudes during evolution. In the process of evolution, the density of unstable dark-gap soliton is not missing, and an upward protrusion is formed, and the amplitude of oscillation waves is different.

Figure 2(c) shows the separation distance between adjacent dark-gap solitons ($\Delta_l = \pi$) is equal to half of the period of the mixed lattice. Further studies have find that multipole dark-gap solitons can also exist stably at different separation distances. Figures 6(a) and 6(b) are the separation distance $\Delta_l = 2\pi$ and 4π waveforms. Their waveforms change in the

same way as fundamental dark-gap solitons. We find that the structure of these dark-gap solitons does not cause background changes.

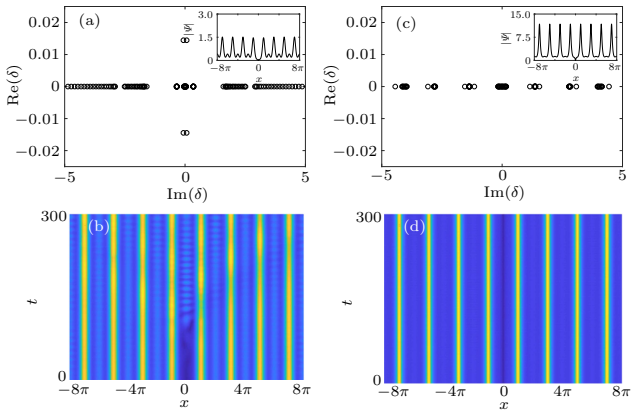


Fig. 5. Linear stability analysis (top) and real-time evolution (bottom) in the linear and nonlinear lattices with different periodic distributions. Panels (a) and (b) represent an unstable fundamental dark-gap soliton at $v_0 = 3.0$, $\mu = 1.16$. Panels (c) and (d) indicate a stable fundamental dark-gap soliton with $v_0 = 3.0$, $\mu = 3.70$. The inner diagrams of panels (a) and (c) are their corresponding solitons profile.

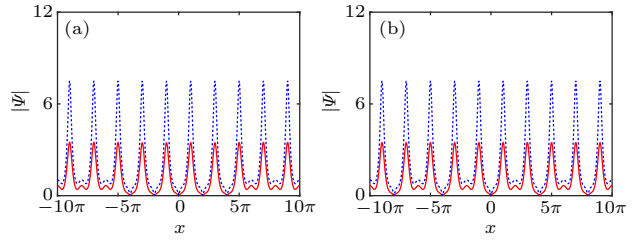


Fig. 6. Profiles of fivepole dark-gap solitons in linear and nonlinear lattices with different periodic distributions. Panels (a) and (b) are $v_0 = 3.0$, $w_0 = 1.0$, $\mu = 1.50$ (solid red line), and $\mu = 2.50$ (dotted blue line).

Next, we change the defective atomic number N and chemical potential μ of these two fivepole dark-gap solitons in Fig. 7(a). In the band gap, the N increases with the increase of μ, but the slope is larger in the first band gap. Compared to the fivepole dark-gap solitons in Fig. 3(a), their numbers are not particularly large. The relationship between $\mathrm{Re}(\delta)$ and μ is obtained by linear stability analysis at $v_0 = 3.0$. The results show that the stability of the fivepole dark-gap solitons in Fig. 7(b) is greater than that of the fivepole dark-gap solitons in Fig. 3(b). All solitons are stable, except at the first gap edge, which is unstable. Our simulations show that such multipole solitons can only be robustly stable if the spacing between neighboring solitons is greater than or equal to their periods.

When the linear lattice depth of the fivepole dark-gap soliton is increased to $v_0 = 6.0$, it is clearly found that the stability of the soliton in the band gap is enhanced. We try to increase the nonlinear lattice amplitude $w_0 = 2.0$, and the results are in high agreement with Fig. 4(b) that there are no solitons in the band gap. When the linear and nonlinear regions lie in the same period, $W = w_0 \cos(2x)$, the solitons in the first band gap are stable except for the band gap edges which have unstable solitons corresponding to the chemical potential μ, and the stability of the solitons is weakened and the solitons are roughly all unstable in the second band gap. Therefore, we find that changes in the linear part increase the stability of the soliton, while changes in the nonlinear part decrease the stability of the soliton in this paper.

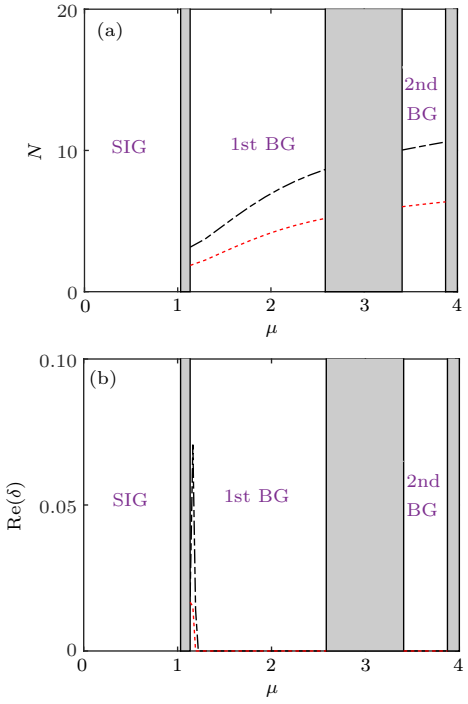


Fig. 7. The defective atomic number N (top) and the real part $\mathrm{Re}(\delta)$ of the eigenvalue (bottom) *versus* chemical potential μ for fivepole dark-gap solitons. The dashed black and dotted red lines correspond to solitons in Figs. 5(a) and 5(b), respectively. The parameters of panels (a) and (b) are $v_0 = 3.0$, $w_0 = 1.0$. The blank spaces represent the band gaps, and shaded areas represent energy bands. SIG and 1st (2nd) BG are semi-infinite band gap, first (second) band gap.

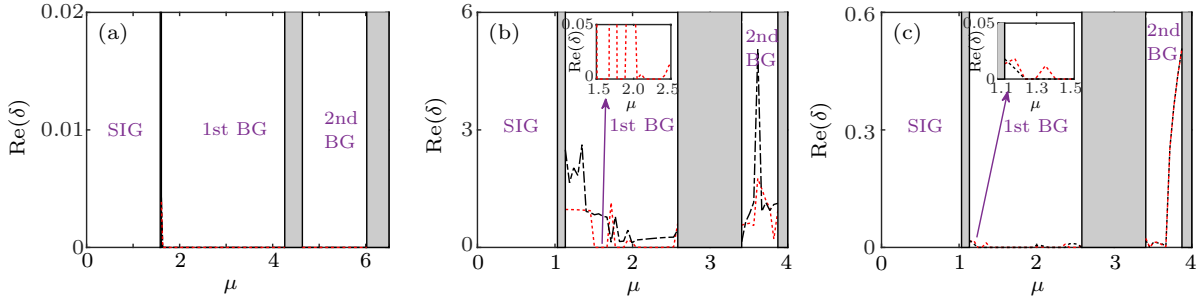


Fig. 8. The relationship between the real part $\mathrm{Re}(\delta)$ of the eigenvalue of fivepole dark-gap solitons and the chemical potential μ: (a) $v_0 = 6.0$, $w_0 = 1.0$; (b) $v_0 = 3.0$, $w_0 = 2.0$, and (c) $v_0 = 3.0$, $w_0 = 1.0$, $W = w_0 \cos(2x)$.

As shown in Fig. 9, we validated the linear stability analysis relationship in Fig. 7(b). The stable and unstable solitons in the black line are randomly selected to verify that their stability is correct. In any imaginary part $\mathrm{Im}(\delta)$, the stable soliton has a real part $\mathrm{Re}(\delta) = 0$, and the soliton remains unchanged during evolution. The real part of the unstable soliton $\mathrm{Re}(\delta) \neq 0$ and the amplitude change of the soliton during evolution and oscillates around $x = 0$. We find that the linear stability analysis is highly consistent with real-time evolution.

When the nonlinear lattice is $W = w_0 \cos(2x)$, where the periods of both the linear and nonlinear lattices are π. The depth of the linear lattice is fixed at $v_0 = 3.0$. We find that the continuous wave background in this case is somewhat different from the background state above. The period of the background is π and the background amplitude is the same throughout the interval. Comparisons of Figs. 3(d) and 4(c) reveal that the dark-gap solitons of linear and nonlinear lattices with different periods are more stable than those with the same period.

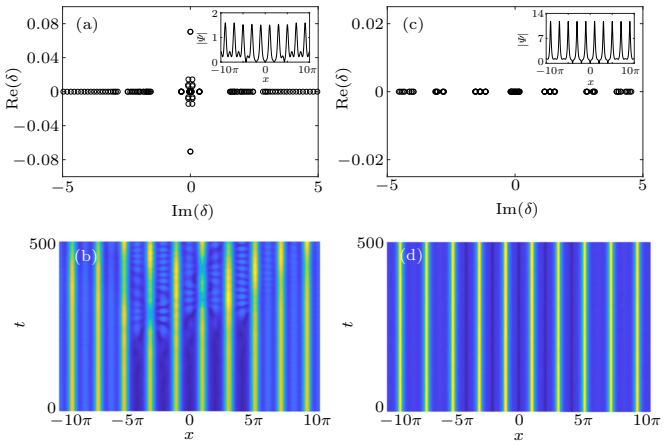


Fig. 9. Linear stability analysis (top) and real-time evolution diagram (bottom) of the separation distances $\Delta_l = 2\pi$ fivepole dark-gap solitons. An unstable dark-gap soliton at $v_0 = 3.00$, $\mu = 1.17$ in panels (a) and (b). Panels (c) and (d) indicate a stable dark-gap soliton with $v_0 = 3.0$, $\mu = 3.70$. The inner diagrams of panels (a) and (c) are their corresponding solitons profile.

4. Conclusion

Dark-gap solitons can be generated in linear lattice and nonlinear lattice systems. Under the spatial distribution of different periodic periods, the background wave have two different amplitudes in one period. By varying the linear lattice depth, the nonlinear lattice amplitude, and the nonlinear lattice period, we find that the amplitude of the dark-gap solitons and the size of the cup-shaped portions show regular changes. The stable and unstable regions of the fundamental dark-gap solitons in the band gap are determined by two different methods. The stabilization region of its soliton expands with increasing lattice depth, on the contrary, the change in the nonlinear part decreases the stability of the soliton whether the nonlinear lattice amplitude or the period of the nonlinear lattice is changed. By changing the distance between adjacent solitons, three kinds of fivepole dark-gap solitons that can exist stably are found. When the distance between the adjacent solitons is π, the tripole and fivepole dark-gap solitons partially exist stably in the band gap; when the distances between adjacent solitons are 2π and 4π, the fivepole dark-gap solitons are approximately all stable in the band gap. Therefore, solitons are more stable when the distance between adjacent solitons is greater than or equal to their total period.

Acknowledgement

Project supported by the Innovation Capability Improvement Project of Hebei Province, China (Grant No. 22567605H).

References

[1] Gibbon J D 1973 *Soliton Solutions of Non Linear Wave Equations and Some Related Problems in Linear and Non-Linear Optics* (University of Manchester)
[2] Elgin J N 1993 *Phys. Rev. A* **47** 4331
[3] Krämer M, Pitaevskii L and Stringari S 2002 *Phys. Rev. Lett.* **88** 180404
[4] Combescot M, Combescot R and Dubin F 2017 *Rep. Prog. Phys.* **80** 066501
[5] Burger S, Bongs K, Dettmer S, Ertmer W, Sengstock K, Sanpera A, Shlyapnikov G V and Lewenstein M 1999 *Phys. Rev. Lett.* **83** 5198
[6] Becker C, Stellmer S, Soltan-Panahi P, Dörscher S, Baumert M, Richter E, Kronjäger J, Bongs K and Sengstock K 2008 *Nat. Phys.* **4** 496
[7] Wen J M, Bo W B, Wen X K and Dai C Q 2023 *Acta Phys. Sin.* **72** 100502 (in Chinese)
[8] Biancalana F, Amann A and O'Reilly E P 2008 *Phys. Rev. A* **77** 011801
[9] Grigoriev V V and Biancalana F 2010 *Photonic Nanostruct.* **8** 285
[10] Aceves A B, Fibich G and Ilan B 2004 *Physica D* **189** 277
[11] Otsobo J A A, Megne L T, Tabi CB and Kofané TC 2022 *Chaos, Solitons and Fractals* **158** 112034
[12] Yang J and Zhang Y P 2023 *Phys. Rev. A* **107** 023316
[13] Pang F Z, Gegen H and Zhao X M 2023 *Chin. Phys. B* **32** 050205
[14] Li P P, Zhao Y, Xu S L, Zhou Q, Fu Q D, Ye F W, Hua C P, Chen M W, Hu H J and Zhou Q Q 2023 *Chin. Phys. Lett.* **40** 28
[15] Cerda-Méndez E A, Sarkar D, Krizhanovskii D N, Gavrilov S S, Biermann K, Skolnick M S and Santos P V 2013 *Phys. Rev. Lett.* **111** 146401
[16] Busch T and Anglin J R 2000 *Phys. Rev. Lett.* **84** 2298
[17] Stellmer S, Becker C, Soltan-Panahi P, Richter E M, Dörscher S, Baumert M, Kronjäger J, Bongs K and Sengstock K 2008 *Phys. Rev. Lett.* **101** 120406
[18] Weller A, Ronzheimer J P, Gross C, Esteve J, Oberthaler M K, Frantzeskakis D J, Theocharis G and Kevrekidis P G 2008 *Phys. Rev. Lett.* **101** 130401
[19] Pedri P and Santos L 2005 *Phys. Rev. Lett.* **95** 200404
[20] Shomroni I, Lahoud E, Levy S and Steinhauer J 2009 *Nat. Phys.* **5** 193
[21] Frantzeskakis D J 2010 *J. Phys. A: Math. Theor.* **43** 213001
[22] Kevrekidis P G, Frantzeskakis D J and Carretero-González R 2015 *SIAM*
[23] Tsitoura F, Anastassi Z A, Marzuola J L, Kevrekidis P G and Frantzeskakis D J 2016 *Phy. Rev. A* **94** 063612
[24] Sciacca M, Barenghi C F and Parker N G 2017 *Phys. Rev. A* **95** 013628
[25] Liu W J, Huang L G, Huang P, Li Y Q and Lei M 2016 *Appl. Math. Lett.* **61** 80
[26] Zhou Q, Xu, M Y, Sun Y Z, Zhong Y and Mirzazadeh M 2022 *Nonlinear Dyn.* **110** 1747
[27] Li S R, Bao Y Y, Liu Y H and Xu T F 2022 *Chaos, Solitons and Fractals* **162** 112484
[28] Li X Y, Qi J J, Zhao D and Liu W M 2023 *Acta Phys. Sin.* **72** 106701 (in Chinese)
[29] Bao Y Y, Li S R, Liu Y H and Xu T F 2022 *Chaos, Solitons and Fractals* **156** 111853

[30] Alexander T J, Tsolias G A, Demirkaya A, Decker R J, Martijn de Sterke C and Kevrekidis P G 2022 *Opt. Lett.* **47** 1174
[31] He T and Wang Y Y 2021 *Appl. Math. Lett.* **121** 107405
[32] Paredes A, Salgueiro J R and Michinel H 2022 *Physica D* **437** 133340
[33] Zeng J H and Malomed B A 2012 *Phys. Rev. A* **85** 023824
[34] Zeng L W and Zeng J H 2019 *Adv. Photon. Res.* **1** 046004
[35] Xie Q T 2021 *Results Phys.* **28** 104575
[36] Hong J, Wang C H and Zhang Y P 2023 *Phys. Rev. E* **107** 044219
[37] He Y J, Zhu X, Mihalache D, Liu J L and Chen Z X 2012 *Phys. Rev. A* **85** 013831
[38] He Y J, Zhu X, Mihalache D, Liu J L and Chen Z X 2012 *Opt. Commun.* **285** 3320
[39] Brazhnyi V A and Konotop V V 2004 *Mod. Phys. Lett. B* **18** 627
[40] Zeng L W and Zeng J H 2019 *Opt. Lett.* **44** 2661
[41] Li J W, Zhang Y P and Zeng J H 2022 *Chaos, Solitons and Fractals* **157** 111950
[42] Zeng L W, Shi J C, Li J W, Li J Z and Wang Q 2022 *Opt. Express* **30** 42504
[43] Dasgupta R, Venkatesh B P and Watanabe G 2016 *Phys. Rev. A* **93** 063618
[44] Zhang S L, Zhou Z W and Wu B 2013 *Phys. Rev. A* **87** 013633
[45] Li J W and Zeng J H 2021 *Phys. Rev. A* **103** 013320
[46] Ma J P, Wang Q Q, Tu P, Shao K H, Zhao Y X, Su R M, Zhao X, Xi B L and Shi Y R 2024 *Phys. Scr.* **99** 045251
[47] Zhou Y S, Meng H J, Zhang J, Li X L, Ren X P, Wan X H, Zhou Z K, Wang J, Fan X B and Shi Y R 2021 *Sci. Rep.* **11** 11382
[48] Strecker K E, Partridge G B, Truscott A G and Hulet R G 2002 *Nature* **417** 150
[49] Wu S L, Huang C M and Liu Y 2008 *Appl. Math. Comput.* **201** 553
[50] Zhang Y P, Liang Z X and Wu B 2009 *Phys. Rev. A* **80** 063815
[51] Cao Y and Xu T F 2023 *Phys. Rev. A* **108** 013509